Fixed switching frequency scheme for current predictive control of DFIG

ARIA YOUNESI[1], **SAJAD TOHIDI**[1,*], **AND MOHAMMAD REZA FEYZI**[1]

[1] *Faculty of electrical and computer engineering, University of Tabriz, Tabriz, Iran*
[*] *Corresponding author: stohidi@tabrizu.ac.ir*

Manuscript received 05 March, 2021; revised 02 June, 2021; accepted 21 June, 2021. Paper no. JEMT-2103-1286.

This paper suggests a new current predictive control algorithm for the wind-driven doubly-fed induction generator (DFIG) based on space vector modulation (SVM) with fixed switching frequency. Combining the current predictive controller and SVM has the benefits of a predictive controller, and fixing the switching frequency improves the output waveform quality. However, if classical predictive control is used, the computational burden will still be high. The proposed algorithm uses SVM to fix the switching frequency of the rotor side converter. Additionally, by using an incremental algorithm, the proposed technique prevents examining all inputs over the prediction horizon. As a result, in the proposed current predictive algorithm the computational time is significantly reduced. The detailed state-space model of DFIG and rotor side converter are used to execute the predictive algorithm. The proposed algorithm uses the rotor current to predict the next behavior of the DFIG, and then, by using SVM, the duty cycles of 2-level voltage source inverter are obtained. Finally, the proposed controller's responses are compared to those of the SVM-based field-oriented control strategy. Simulation results of the proposed controller on a two-level voltage source inverter under a balanced three-phase power system illustrate the satisfactory active and reactive power tracking and improved quality of the inverter outputs.

keywords: *Current predictive control; fixed switching frequency; space vector modulation; doubly fed induction generator.*

http://dx.doi.org//10.22109/jemt.2021.276331.1286.

NOMENCLATURE

Nomenclature

P_T Wind turbine output power.
ρ Air density.
A_T Rotor swept area.
r_T Blade radius.
v_w Wind speed.
C_P Power coefficient of the rotor blades.
β Pitch angle.
λ_T Optimal TSR.
λ_I Intermittent TSR.
r_{gb} Gearbox ratio.
n_m Generator speed.
n_T Turbine speed.
$v_{s,dq}, v_{r,dq}$ Stator and rotor voltage vectors.
$i_{s,dq}, i_{r,dq}$ Stator and rotor current vectors.
$\psi_{s,dq}, \psi_{r,dq}$ Stator and rotor flux vectors.
R_s, R_r Stator and rotor winding resistance.
ω_s Synchronous speed.
ω_r Electrical rotor speed.
$\omega_s l$ Slip angular speed.
L_{ls}, L_{lr} Stator and rotor leakage inductances.
L_s, L_r Stator and rotor self-inductances.
L_m Magnetizing inductance.
T_e Electromagnetic torque.
P_P Number of pole pairs.
P_s, Q_s Stator active and reactive powers.
$A(t)$ State matric in continuous-time mode.
$\boldsymbol{B}$ Input matric in continuous-time mode.
T_s Control sampling time.
$\Phi(k)$ State matric in discrete-time mode.
Γ Input matric in discrete-time mode.
$\boldsymbol{I}$ Unity matrix.
$\boldsymbol{k}$ Sample.
$v^p_{s,dq}, v^p_{r,dq}$ Predicted stator and rotor voltage vectors.
$i^p_{s,dq}, i^p_{r,dq}$ Predicted stator and rotor current vectors.

$v_{dc}(k)$ Measured DC link voltage.

$s_{dr}^{p}(k), s_{qr}^{p}(k)$ Eight possible switch position combinations of the RSC (d, q axis, respectively).

J Cost function.

P_d, P_q Weighting factors.

1. INTRODUCTION

Nowadays, high greenhouse gas emissions due to fossil fuels are known as a global problem. Therefore, renewable energy sources play an essential role in global energy production [1]. However, the wind is more attractive due to its rapid development and cost-effectiveness [2, 3].

Today, variable speed wind turbines are used extensively due to the many advantages over the fixed speed ones. In the meantime, limited variable speed turbines with DFIG, due to fractionally-rated power converters, resulting in relatively low initial costs. Their ability to independently active and reactive power control through feeding the rotor currents has become very popular in the industry. Hence, more than 70 percent of today's turbines are variable speed types with DFIG [4, 5].

Various control methods have been presented for DFIG. In [6–8], vector-based control and field-oriented control techniques are used to control the DFIG. Such methods control the output powers of DFIG by controlling the rotor currents. However, in these methods, despite the system's proper performance in the steady-state, due to the cascade structure of the proportional-integral (PI) controllers, they are sensitive to changes in the machine parameters. They have inadequate dynamic response [9, 10]. In [11], direct torque control (DTC) based on hysteresis band and switching table are presented. In [12, 13], this method controls the rotor side converter in DFIG. However, this method simplifies DFIG control, but variable and high switching frequency, the high oscillation of torque, and the need for two switching tables are disadvantages of this method [14, 15]. Such have a complicated design and requires the exact adjustment of the modulator's time. Also, due to the use of PI controllers, their dynamic are lower than conventional DTC.

Today, new controllers have been proposed based on fuzzy, and adaptive control, and sliding mode control. In [16], an adaptive virtual inertia controller for DFIGs is proposed. In this nonlinear control method, the aerodynamic efficiency is considered. In [17, 18], comprehensive direct power control with vector control methods for DFIG are proposed. A multimode controller for a DFIG is proposed in [19]. Fuzzy-based controllers for DFIG connected to the wind turbine are presented in [2, 20, 21]. In [22, 23], sliding mode-based strategies are proposed for controlling the power of DFIG. Such methods achieve significant DFIG control improvements, but most of them still need a cascade loop to hold and therefore have limited bandwidth [24, 25].

In recent years, predictive control-based methods have attracted more attention in the power converters and electric drive systems. [26, 27]. In model predictive control by using an explicit model the next behavior of the system is predicted, and finally the control system output is obtained by solving an optimization problem [28, 29]. A time efficient model predictive control method for DFIG is proposed in [30]. Here, the switching states of the converter are considered as the control inputs of the predictive controller. In [31, 32], robust finite control set model predictive control are proposed. In [31], a term is added to the predicted rotor voltages for considering the mistakes due to parameters' estimation, and in [32], by using a matrix converter a model predictive rotor current control is proposed. To quality improvement of an electrical network a novel method that derives the power coefficient based on DFIG is proposed [33]. In [34], a model-free predictive control for a DFIG is presented in which an ultra-local model is used to replace the mathematical model of the plant. In [35], an effective sensor-less model predictive voltage control is used for a DFIG. Also, in [36], a continuous-time model predictive control is used for DFIG. Taylor series expansion is used to predict the current. All the above-mentioned methods have an excellent dynamic response and lowers the torque fluctuations, but they still need an accurate calculation of each voltage vector's time interval, and they are very complex.

Direct predictive current control with pulse width modulation at low switching frequency is presented for a high power DFIG [37]. A robust model predictive control is proposed to reduce the torque oscillation in DFIG [38]. In [39], flux weakening control by flux linkage prediction controls the rotor flux during grid voltage dips. In [40], an overview of DFIG fault ride through methods is presented. By reducing the control inputs, linearization or raising the sampling frequency solutions are suggested in all these methods. In [41], the rotor side converter's Switching frequency has been fixed by using SVM. However, the main problem is that it can only be implemented at low switching frequencies (below 1kHz). A model predictive direct power control with a three-level inverter is presented in [42]. Good results can be seen by fixing the switching frequency. Nevertheless, in this paper, similar to other predictive-based methods, the real-time evaluation is high. Therefore, the authors have been forced to decrease the degree of freedom of the controller, and only combinations are selected that have one switching variation in each step.

Since the wind intensity is always changing, the DFIG output must also be continuously adjusted to track its reference value. Control goals in the doubly fed induction generator are divided into two categories. The main goal is chasing the power and the second goal is to limit the rotor current when the voltage drop occurs [38]. Therefore, it is suggested to utilize a predictive control-based method to respond to both the problem in the best way. The proposed strategy utilizes the space vector modulation to fix the inverter switching frequency. Combining the current predictive controller and SVM has the benefits of two methods together. Also, it is suggested to use an incremental algorithm to reduce the computational time of predictive control implementation. The main contribution of this paper is to use a new current predictive control algorithm for the wind-driven DFIG. The detailed state-space model of DFIG and rotor side converter are used to execute the predictive algorithm. The proposed algorithm predicts the rotor current to estimate the future behavior of the DFIG, and then, by using SVM, the duty cycles are obtained. Using the current control in the synchronous reference frame, the proposed controller directly controls the active and reactive power of the DFIG. Thus, the online solving of the problem is straightforward and considers any constraint for the parameters. Finally, the main contribution of the suggested strategy can be summarized as follows:

- By using SVM, the switching frequency of the inverter can be fix
- The SVM's calculations are performing in the prediction
- To reduce the computational burden of the proposed tech-

nique, an incremental algorithm is used in the online optimization process

2. MODELING OF SYSTEM

A. Wind Turbine

According to [43],The following achieves the wind turbine output power

$$P_T = P_w \times C_p = \frac{1}{2}\rho A_T v_w^3 C_p \quad (1)$$

C_p represents the rotor blades' power coefficient, which ranges from 0.32 to 0.52 in practical wind turbines. C_p could be defined as below

$$C_p = C_1\left(\frac{C_2}{\lambda_I} - C_3\beta - C_4\beta^2 - C_5\right)e^{-\frac{C_6}{\lambda_I}} + C_7\lambda_T \quad (2)$$

where λ_T is the optimal tip-speed ratio (O-TSR) and λ_I is intermittent TSR and is related to λ_T and β. λ_T and λ_I are defined as:

$$\lambda_T = \lambda_T^{opt} = \frac{\omega_T \times r_T}{v_{w,rated}} \quad (3)$$

$$\frac{1}{\lambda_I} = \frac{1}{\lambda_T + 0.08\beta} - \frac{0.035}{\beta^3 - 1} \quad (4)$$

The gearbox ratio is calculated according to the rated speed of the wind turbine and generator that is

$$r_{gb} = \frac{n_m}{n_T} \quad (5)$$

Where n_m and n_T are the generator and turbine speed, respectively. The ratio is equal to 1 for a direct-drive turbine, and it is 96 for the studied DFIG [43].

B. Dynamic model of DFIG

The predictive control method utilizes the DFIG and rotor side converter (RSC) mathematical model to predictor currents' future behaviors. According to [43], the stator and rotor voltage vectors are defined as

$$\mathrm{v_{s,dq}} = R_s \mathrm{i_{s,dq}} + \frac{d}{dt}\psi_{\mathrm{s,dq}} + j\omega_s \psi_{\mathrm{s,dq}} \quad (6)$$

$$\mathrm{v_{r,dq}} = R_r \mathrm{i_{r,dq}} + \frac{d}{dt}\psi_{\mathrm{r,dq}} + j\left(\omega_s - \omega_r\right)\psi_{\mathrm{r,dq}} \quad (7)$$

Where ω_s is the synchronous speed, and is the electrical rotor speed. The slip angular velocity is defined $\omega_{sl} = (\omega_s - \omega_r)$. During the steady-state operation, the stator flux is obtained by

$$P_T = P_w \times C_p = \frac{1}{2}\rho A_T v_w^3 C_p \quad (8)$$

Also, the stator and rotor flux linkage vectors are expressed as follow

$$\psi_{\mathrm{s,dq}} = L_s \mathrm{i_{s,dq}} + L_m \mathrm{i_{r,dq}} \quad (9)$$

$$\psi_{\mathrm{r,dq}} = L_r \mathrm{i_{r,dq}} + L_m \mathrm{i_{s,dq}} \quad (10)$$

where

$$L_s = L_{ls} + L_m \quad (11)$$

$$L_r = L_{lr} + L_m \quad (12)$$

The electromagnetic torque is

$$T_e = \frac{3P_p L_m}{2\omega_s L_s}\left(-i_{qr}v_{qs} + R_s i_{qs} i_{qr} + R_s i_{ds} i_{dr} - i_{dr} v_{ds}\right) \quad (13)$$

The DFIG stator powers can be calculated by

$$P_s = \frac{3}{2}(v_{ds} i_{ds} + v_{qs} i_{qs}) \quad (14)$$

$$Q_s = -\frac{3}{2}(v_{qs} i_{ds} - v_{ds} i_{qs}) \quad (15)$$

Regarding the equations mentioned above, the rotor currents are expressed in terms of stator active and reactive powers [44, 45], as:

$$i_{dr} = -\left(\frac{2L_s}{3v_{ds}Lm}\right)P_s - \left(\frac{R_s}{\omega_s L_m}\right)i_{qs} \quad (16)$$

$$i_{qr} = +\left(\frac{2L_s}{3v_{ds}Lm}\right)Q_s + \left(\frac{R_s}{\omega_s L_m}\right)i_{ds} - \left(\frac{1}{\omega_s L_m}\right)v_{ds} \quad (17)$$

Since the stator resistance is low, it is concluded that the active power and reactive power of the stator can be controlled independently.

3. CURRENT PREDICTIVE CONTROL WITH SVM FOR DFIG

Fig. 1 shows the DFIG-based wind power system with the proposed predictive controller considered in this paper. In the proposed scheme, the rotor currents in $\alpha\beta$ the reference frame are the current predictive control results, and then, by using SVM, the duty cycles of 2-level voltage source inverter (T_a, T_b, T_c) are obtained. Finally, the on-off switch states are applied through a PWM.

A. Current Predictive Control

The state-space dynamic model of rotor and stator currents, stated in 18, is used to design the current predictive control scheme.

$$\frac{d}{dt}\begin{bmatrix} i_{ds} \\ i_{qs} \\ i_{dr} \\ i_{qr} \end{bmatrix}_{4\times1} = k_\sigma [A(t)]_{4\times4}\begin{bmatrix} i_{ds} \\ i_{qs} \\ i_{dr} \\ i_{qr} \end{bmatrix}_{4\times1} + k_\sigma [B]_{4\times4}\begin{bmatrix} v_{ds} \\ v_{qs} \\ v_{dr} \\ v_{qr} \end{bmatrix}_{4\times1} \quad (18)$$

where $A(t)$ and B are the state and input matrices, with the following values

$$A(t) = k_\sigma \begin{bmatrix} -R_s L_r & \omega_r L_m^2 + k_\omega & R_r L_m & \omega_r L_m L_r \\ -\omega_r L_m^2 - k_\omega & -R_s L_r & -\omega_r L_m L_r & R_r L_m \\ R_s L_m & -\omega_r L_m L_s & -R_r L_s & -\omega_r L_r L_s + k_\omega \\ \omega_r L_m L_s & R_s L_m & \omega_r L_r L_s - k_\omega & -R_r L_s \end{bmatrix}$$

$$\mathrm{B} = k_\sigma \begin{bmatrix} L_r & 0 & -L_m & 0 \\ 0 & L_r & 0 & -L_m \\ -L_m & 0 & L_s & 0 \\ 0 & -L_m & 0 & L_s \end{bmatrix}$$

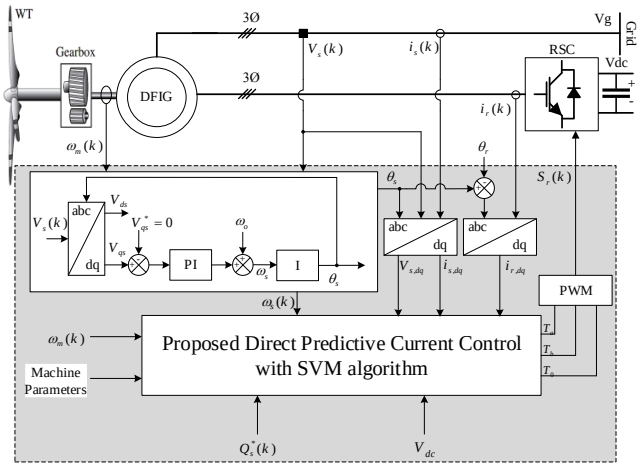

Fig. 1. The DFIG-based wind power system with the proposed controller.

Where $k_\sigma = \left(\frac{1}{\sigma L_s L_r}\right)$ and $[k_\omega = \omega_s \sigma L_s L_r]$.
To predict the next sampling time (k+1), the discrete-time dynamic model is required. Assuming that T_s is the control sampling time, $\Phi(k)$ and Γ are the state and input matrices in discrete-time, the correlation between the discrete-time and continues-time matrices can be defined as:

$$\Phi(k) = (\mathrm{I} + A(t)T_s), \Gamma = BT_s \tag{19}$$

Where I is the unity matrix.
Therefore, the DFIG rotor and stator currents are predicted by the following equations:

$$\begin{bmatrix} i_{ds}^p(k+1) \\ i_{qs}^p(k+1) \\ i_{dr}^p(k+1) \\ i_{qr}^p(k+1) \end{bmatrix}_{4\times1} = [\Phi(k)]_{4\times4} \begin{bmatrix} i_{ds}(k) \\ i_{qs}(k) \\ i_{dr}(k) \\ i_{qr}(k) \end{bmatrix}_{4\times1} + [\Gamma]_{4\times4} \begin{bmatrix} v_{ds}(k) \\ v_{qs}(k) \\ v_{dr}^p(k) \\ v_{qr}^p(k) \end{bmatrix}_{4\times1} \tag{20}$$

where $[v_{dr}^p(k)]$ and $[v_{qr}^p(k)]$ are the predicted rotor voltages, calculated as:

$$\begin{bmatrix} v_{dr}^p(k) \\ v_{qr}^p(k) \end{bmatrix}_{2\times1} = v_{dc}(k) \begin{bmatrix} s_{dr}^p(k) \\ v_{qr}^p(k) \end{bmatrix}_{2\times1} \tag{21}$$

B. Cost function

According to equations 16 and 17, to DFIG active and reactive power control, the RSC's control objective includes the regulation of dq-axes rotor currents. Accordingly, the objective function is defined as:

$$J(k) = P_d(i_{dr}{}^*(k+1) - i_{dr}{}^p(k+1))^2 + P_q(i_{qr}{}^*(k+1) - i_{qr}{}^p(k+1))^2 \tag{22}$$

$[P_d]$ and $[P_q]$ are the weighting factors. During each sampling period, the optimum voltage vector which minimizes the objective function is selected.

C. SVM

After predicting the reference values of stator and rotor currents, the next step is to generate the required switching voltage vector. The space vector modulation technique is the best method among all the pulse with modulation (PWM) techniques [43]. The SVM gives higher voltage amplitude and a better harmonic spectrum. A three-phase 2-level voltage source inverter with V_{dc} as the DC link voltage has only eight possible switch position combinations. In this section, step-by-step implementation of the current predictive control with the SVM algorithm is presented in **Algorithm 1**.
Predictive control based methods could easy handle constraints of the system. In this paper $\sqrt{i_{dr}^2 + i_{qr}^2} \leq I_{r,\max}$ is considered as the main constraition of the system.

4. SIMULATION RESULTS

To validate the proposed control strategy, the performance of a 3-MW DFIG is investigated. The main parameters of the studied system are given in Table 1 [43]. Simulation results are obtained with a detailed model of the machine and test-rig by using MATLAB/Simulink.

A. Steady-state analysis of DFIG

The DFIG is assumed to operate at a unity power factor with $v_w = 9$ m/s (0.75 pu). Fig. 2, shows the slip angle θ_{sl}. Due to the constant wind and generator speed, the slip angle uniformly increases from 0 - 2π. Steady-state waveforms of DFIG operating with the proposed strategy are presented in Fig. 3.
In the top plot of Fig. 3, active and reactive powers of DFIG are shown, which indicates that the DFIG generates 0.5pu as active power and zero reactive power. In the middle plot, voltage, and

Table 1. Main parameters of DFIG system.

DFIG Parameters	
Rated power (kW)	3000
Stator line to line voltages (V)	690
Stator current (A)	2076.2
Rotor line to line voltage (V)	158.7
Rotor current (A)	2673.1
Pole pairs	2
$f_s(Hz)$	60
$R_s(m\Omega)$	1.443
$R_r(m\Omega)$	1.125
$L_{ls}(mH)$	0.094
$L_{lr}(mH)$	0.085
$L_m(mH)$	0.802
$J_m(kg.m^2)$	680
Wind Turbine Parameters	
Rated power (kW)	3000
Gain of the gear box for DFIG	96
The turbine radius (m)	43.36
Turbine constants	
$C1...C_7 = [0.39151160.405210.0192]$	

current of stator phase "a" are shown. As observed, the stator operates in the generating mode at unity power factor (UPF). Finally, in the bottom plot of Fig. 3, the rotor currents are illustrated. It shows the sinusoidal waveforms at the frequency of 5Hz, and there is almost no additional harmonic.

To accurately compare the quality of the proposed strategy's waveforms with previous methods, the phase "a" rotor side converter voltage and the frequency spectrum are shown in Fig. 4. Figs. 4 (a) and (b) show the PI FOC's responses by using PWM. Figs. 4 (e) and (f) show the current predictive controller's responses without SVM. It is observed from such FFT plots that there are additional harmonics in both the FOC and current predictive control methods. Despite many such different harmonics in the current predictive controller, their amplitude is much lower than FOC. Therefore, by reducing the number of additional harmonics, the power quality is enhanced. The phase-a voltage and the spectrum analysis of the current predictive control with SVM are shown in Figs. 4 (g) and (h). Also, Figs. 4 (c) and (d) show the FOC method's response using SVM. According to such plots, current predictive control with SVM results in much better FFT with lower additional harmonics, resulting in superior power quality.

B. Transient analysis of DFIG

In this case, the dynamic performance of the DFIG during a change of rotor speed is investigated. According to the turbine and generator's large inertia, the mechanical part dynamics are much slower than that of electric components in the MW wind turbines. Hence, the generator speed cannot be changed instantaneously. Therefore, a ramp change in wind speed is applied to increase the rotor speed from 0.75 pu (sub-synchronous mode) to 1 pu (super-synchronous mode). Fig. 5 shows the wind speed and the slip angle θ_{sl}. In this test, reactive power is kept constant at zero, while active power varies with the variations of wind speed.

Fig. 5(b), θ_{sl} shows an accelerating nature until the rotor speed reaches the synchronous speed. Then, θ_{sl} exhibits a decelerating character.

In Fig. 6, the transient waveforms of DFIG operating with the proposed controller and FOC-SVM are presented. Fig. 6 (a) indicates the excellent performance of DFIG in active and reactive power tracking by using the proposed strategy with lower overshoots and lower fluctuations.

Fig. 7, shows the rotor speed and the amplitude of rotor currents increases proportionally to the rotor speed. Also, at the rotor speed up to the synchronization speed, the frequency of rotor currents decreases and then changes RSC's power direction, the frequency.

C. Evaluation of proposed strategy

In this section, proposed predictive controller is evaluated in two cases.

First, the case of noise in input and output to investigate the robustness of the proposed controller. In this case, 5% error is added to all the measurements and estimations in the controller. Similar to Fig. 5, a ramp change of rotor speed is applied to the wind turbine. Fig. 8, shows the output power of the DFIG by using the proposed D-PCC-SVM for both noise without noise conditions.

As shown in Fig. 8, the proposed method has a small error in transient conditions. But after reaching the steady state, it tracks the final value with very good accuracy and without errors.

PCC. Fig. 9 shows the output power of the DFIG for the case of step changes in wind speed. As shown, two wind speed steps are applied. The first step is from 0.5 to 1 pu at $t = 1$s and the second one is from 1 to 0.5 pu at $t = 2$s. The specification of proposed strategy and conventional one are listed in Table 2.

Table 2. CONTROL SPECIFICATION OF SIMULATION STEPS.

Drive system	Objective function	Prediction horizon (N_p)	Computational time [0-3 sec], (s)
Conventional D-PCC	Eq. (22)	3	42.34
Proposed D-PCC-SVM	Eq. (22)	3	27.09

Based on Table 2, by using the proposed technique the computational burden of the system has reduced up to 35% compared to conventional D-PCC.

5. CONCLUSIONS

In this paper, a new predictive-based controller for DFIG is proposed. The proposed controller utilizes space vector modulation

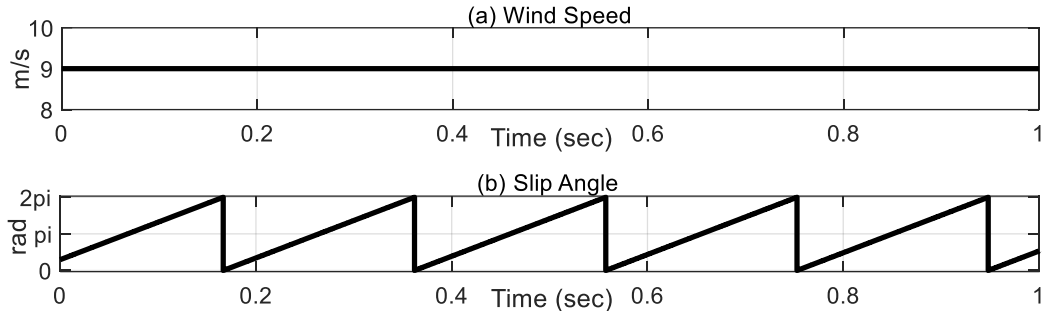

Fig. 2. (a) wind Speed and (b) slip angle of studied wind turbine.

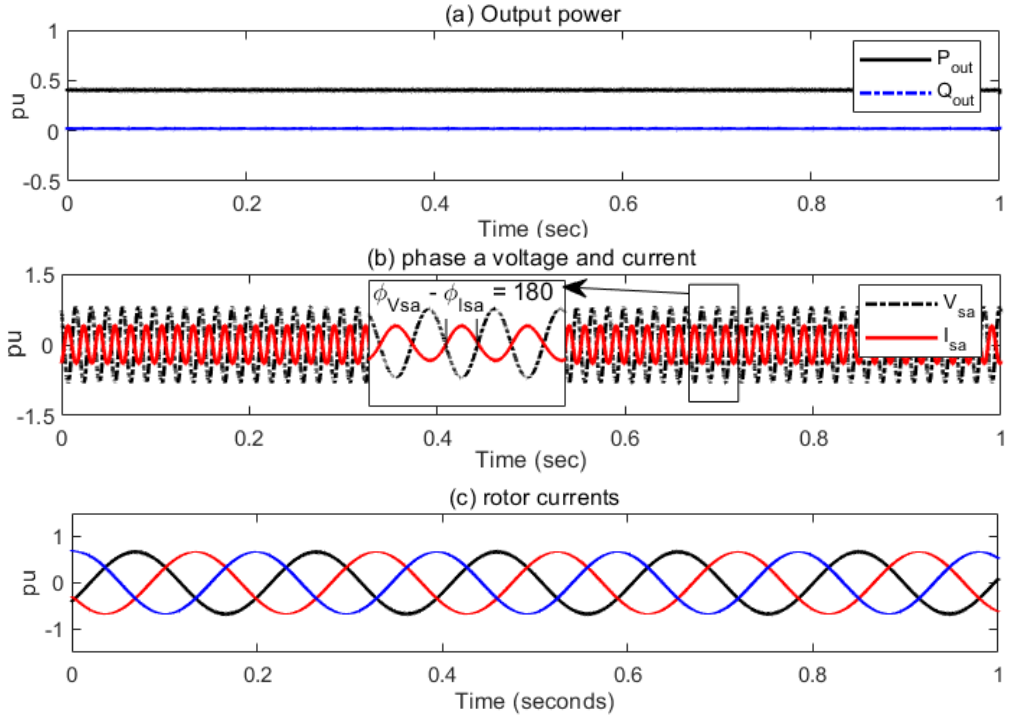

Fig. 3. Steady state waveforms of DFIG. (a) Output active power and reactive power, (b) stator voltage and current of phase "a" and (c) three phase rotor currents.

to fix the switching frequency of RSC. A new incremental algorithm based on the combination of current predictive control and SVM is offered to implement the proposed strategy. The results show fixed switching frequency for DFIG with adequate active power and reactive power tracking. Comparison of the proposed method's responses with those of FOC-SVM strategy shows better FFT with lower additional harmonics, which means superior power quality by using the proposed approach. Moreover, the proposed current predictive control with SVM achieves high quality for the output currents of RSC.
The advantages of suggested strategy against conventional predictive control and FOC-SVM can be summarized as follows:
Proposes predictive control vs conventional predictive control

- Fix switching frequency
- Lower computational burden
- Lower overshoots
- Fast dynamic response

Proposes predictive control vs FOC-SVM

- Better FFT
- Lower additional harmonics
- Faster dynamic response
- Lower overshoots"

REFERENCES

1. A. Erfani, R. Ghasempour, and H. Oraee, "Issue in the Technology Selection for a Wind Farm in Iran," (in en), Journal of Energy Management and Technology, vol. 1, no. 1, pp. 71-78, 2017.

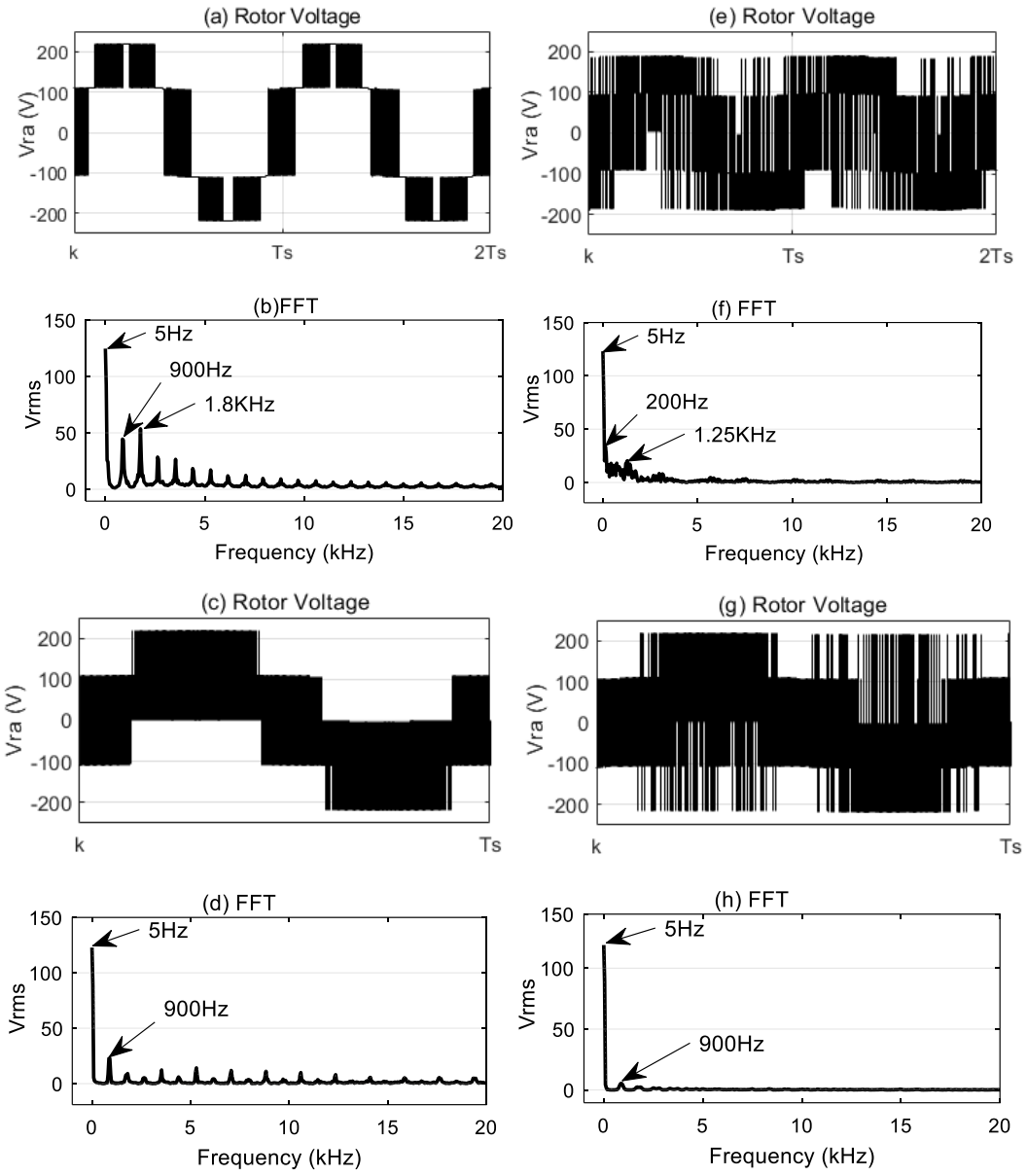

Fig. 4. Phase-a voltage of RSC and spectrum analysis, (a) and (b): responses of FOC without SVM, (c) and (d): responses of FOC with SVM, (e) and (f): responses of D-PCC without SVM and (g) and (h): responses of D-PCC with SVM.

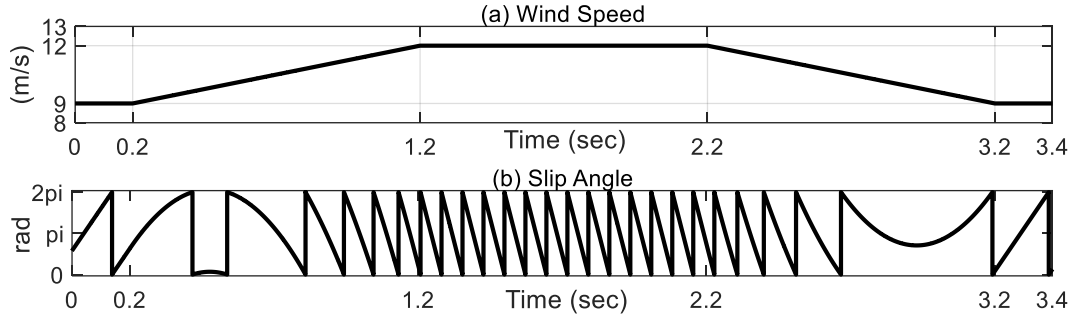

Fig. 5. wind speed and slip angle during the variation of wind speed.

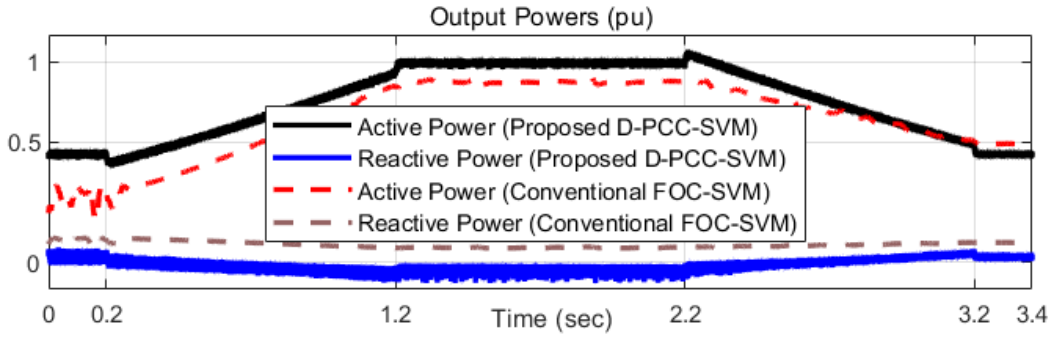

Fig. 6. Output active and reactive power of the proposed strategy and the conventional FOC-SVM.

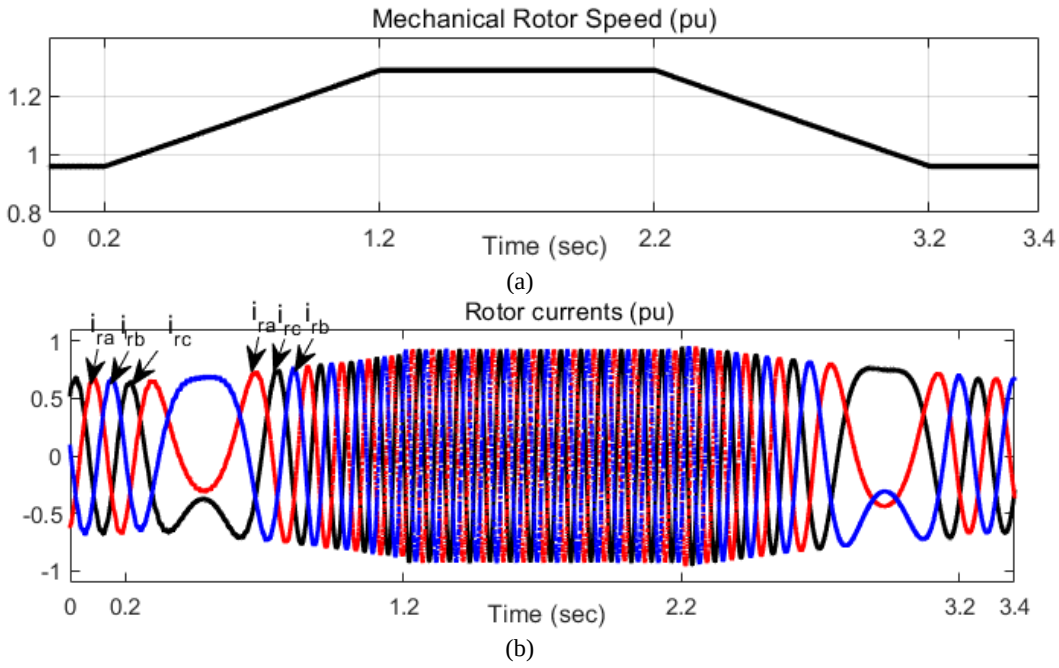

Fig. 7. Transient wave forms of the DFIG. (a) Mechanical rotor speed of the DFIG using the proposed method, (b) Three phase rotor currents of the DFIG with proposed technique.

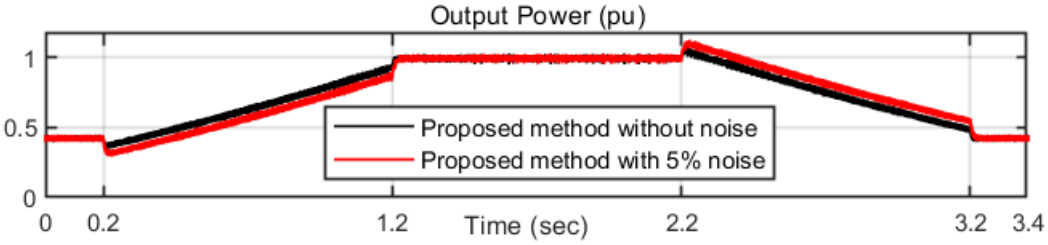

Fig. 8. The output powers of the DFIG using proposed D-PCC-SVM for noise in input and noise in output.

2. R. Pour Ebrahim, S. Tohidi, and A. Younesi, "Sensorless Model Reference Adaptive Control of DFIG by Using High Frequency Signal Injection and Fuzzy Logic Control," (in eng), Iranian Journal of Electrical and Electronic Engineering, Research Paper vol. 14, no. 1, pp. 11-21, 2018.
3. M. Hosseinabadi and H. Rastegar, "DFIG Based Wind Turbines Behavior Improvement during Wind Variations using Fractional Order Control Systems," (in eng), Iranian Journal of Electrical and Electronic Engineering, Research Paper vol. 10, no. 4, pp. 314-323, 2014.
4. A. Younesi, S. Tohidi, and H. Yousefi, "Efficiency maximizing of doubly fed induction generator with considering core loss and reactive power control by optimized model reference adaptive method," Journal of

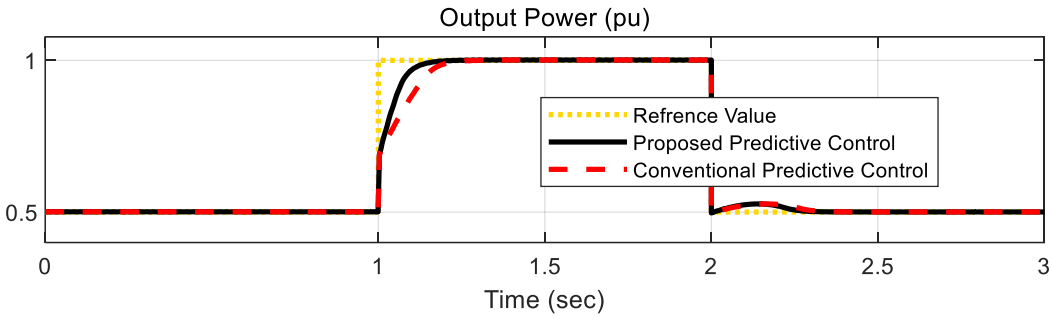

Fig. 9. The output powers of the DFIG using proposed D-PCC-SVM and conventional D-PCC in the case of ramp change in wind speed.

Faculty of Elec., University of Tabriz, vol. 47, no. 2, pp. 791-803, 2017.

5. B. E. Elnaghi, Elkader, F.A., Ismail, M.M., "Adaptation of PI controller used with combination of perturbation and observation method and feedback method for DFIG," Electrical Engineering, vol. 100, no. 2, pp. 1047-1058, 2018.
6. R. Pena, J. C. Clare, and G. M. Asher, "Doubly fed induction generator using back-to-back PWM converters and its application to variable-speed wind-energy generation," IEE Proceedings - Electric Power Applications, vol. 143, no. 3, pp. 231-241, 1996.
7. A. Tapia, G. Tapia, J. X. Ostolaza, and J. R. Saenz, "Modeling and control of a wind turbine driven doubly fed induction generator," IEEE Transactions on Energy Conversion, vol. 18, no. 2, pp. 194-204, 2003.
8. K. K. Jaladi and K. S. Sandhu, "A new hybrid control scheme for minimizing torque and flux ripple for DFIG-based WES under random change in wind speed," International Transactions on Electrical Energy Systems, vol. 0, no. 0, p. e2818.
9. HG. Abad, M. Á. Rodriguez, and J. Poza, "Two-Level VSC Based Predictive Direct Torque Control of the Doubly Fed Induction Machine With Reduced Torque and Flux Ripples at Low Constant Switching Frequency," IEEE Transactions on Power Electronics, vol. 23, no. 3, pp. 1050-1061, 2008.
10. X. Wang and D. Sun, "Three-Vector-Based Low-Complexity Model Predictive Direct Power Control Strategy for Doubly Fed Induction Generators," IEEE Transactions on Power Electronics, vol. 32, no. 1, pp. 773-782, 2017.
11. I. Takahashi and T. Noguchi, "A New Quick-Response and High-Efficiency Control Strategy of an Induction Motor," IEEE Transactions on Industry Applications, vol. IA-22, no. 5, pp. 820-827, 1986.
12. S. Arnalte, J. C. Burgos, and J. L. Rodríguez-Amenedo, "Direct Torque Control of a Doubly-Fed Induction Generator for Variable Speed Wind Turbines," Electric Power Components and Systems, vol. 30, no. 2, pp. 199-216, 2002/02/01 2002.
13. A. Izanlo, Gholamian, S.A. & Kazemi, M.V., "Using of four-switch three-phase converter in the structure DPC of DFIG under unbalanced grid voltage condition," Electrical Engineering, vol. 100, no. 3, pp. 1925-1938, 2018.
14. S. A. Davari, D. A. Khaburi, F. Wang, and R. M. Kennel, "Using Full Order and Reduced Order Observers for Robust Sensorless Predictive Torque Control of Induction Motors," IEEE Transactions on Power Electronics, vol. 27, no. 7, pp. 3424-3433, 2012.
15. F. Niu, K. Li, and Y. Wang, "Direct Torque Control for Permanent-Magnet Synchronous Machines Based on Duty Ratio Modulation," IEEE Transactions on Industrial Electronics, vol. 62, no. 10, pp. 6160-6170, 2015.
16. A. Ashouri-Zadeh and M. Toulabi, "Adaptive Virtual Inertia Controller for DFIGs Considering Nonlinear Aerodynamic Efficiency," IEEE Transactions on Sustainable Energy, vol. 12, no. 2, pp. 1060-1067, 2021.
17. D. Zhi and L. Xu, "Direct Power Control of DFIG With Constant Switching Frequency and Improved Transient Performance," IEEE Transactions on Energy Conversion, vol. 22, no. 1, pp. 110-118, 2007.
18. G. Fei, Z. Tao, and W. Zengping, "Comparative study of direct power control with vector control for rotor side converter of DFIG," in 9th IET International Conference on Advances in Power System Control, Operation and Management (APSCOM 2012), 2012, pp. 1-6.
19. F. A. Bhuiyan and A. Yazdani, "Multimode Control of a DFIG-Based Wind-Power Unit for Remote Applications," IEEE Transactions on Power Delivery, vol. 24, no. 4, pp. 2079-2089, 2009.
20. S. A. E. M. Ardjoun, M. Denai, and M. Abid, "A robust power control strategy to enhance LVRT capability of grid-connected DFIG-based wind energy systems," Wind Energy, vol. 0, no. 0.
21. O. A. Zabin and A. Ismael, "Rotor Current Control Design for DFIG-based Wind Turbine Using PI, FLC and Fuzzy PI Controllers," in 2019 International Conference on Electrical and Computing Technologies and Applications (ICECTA), 2019, pp. 1-6.
22. X. Liu, Y. Han, and C. Wang, "Second-order sliding mode control for power optimisation of DFIG-based variable speed wind turbine," IET Renewable Power Generation, vol. 11, no. 2, pp. 408-418, 2017.
23. D. Sun, X. Wang, H. Nian, and Z. Q. Zhu, "A Sliding-Mode Direct Power Control Strategy for DFIG Under Both Balanced and Unbalanced Grid Conditions Using Extended Active Power," IEEE Transactions on Power Electronics, vol. 33, no. 2, pp. 1313-1322, 2018.
24. M. Preindl and S. Bolognani, "Model Predictive Direct Speed Control with Finite Control Set of PMSM Drive Systems," IEEE Transactions on Power Electronics, vol. 28, no. 2, pp. 1007-1015, 2013.
25. Y. Venkata and W. Bin, "Overview of Digital Control Techniques," in Model Predictive Control of Wind Energy Conversion Systems: Wiley-IEEE Press, 2017, p. 512.
26. J. H. Lee, "Model predictive control: Review of the three decades of development," International Journal of Control, Automation and Systems, journal article vol. 9, no. 3, p. 415, June 04 2011.
27. H. H. H. Mousa, A.-R. Youssef, and E. E. M. Mohamed, "Model predictive speed control of five-phase permanent magnet synchronous generator-based wind generation system via wind-speed estimation," International Transactions on Electrical Energy Systems, vol. 0, no. 0, p. e2826.
28. A. Younesi, S. Tohidi, M. R. Feyzi, and M. Baradarannia, "An improved nonlinear model predictive direct speed control of permanent magnet synchronous motors," International Transactions on Electrical Energy Systems, vol. 28, no. 5, p. e2535, 2018.
29. S. Chikha, "Active and Reactive Power Management of Wind Farm Based on a Six Leg Tow Stage Matrix Converter Controlled by a Predictive Direct Power Controller," (in eng), Iranian Journal of Electrical and Electronic Engineering, Research Paper vol. 14, no. 3, pp. 245-258, 2018.
30. P. Kou, D. Liang, J. Li, L. Gao, and Q. Ze, "Finite-Control-Set Model Predictive Control for DFIG Wind Turbines," IEEE Transactions on Automation Science and Engineering, vol. 15, no. 3, pp. 1004-1013, 2018.
31. A. J. S. Filho, A. L. d. Oliveira, L. L. Rodrigues, E. C. M. Costa, and R. V. Jacomini, "A Robust Finite Control Set Applied to the DFIG Power Control," IEEE Journal of Emerging and Selected Topics in Power Electronics, vol. 6, no. 4, pp. 1692-1698, 2018.

Table 3. Algorithm 1

	Current Predictive Control with SVM algorithm	
1.	Initialize the controller	% Initialization
	Measure the v_s, i_s, i_r	
2.	and the wind speed at the	% Measurements
	k moment	
3.	$g_{op} = \infty, j = 0$	
4.	for j = 1 : 8	
	Current prediction by using (20)	
5.	$i_{dr}^p(k+1), i_{qr}^p(k+1)$	% Prediction
	$i_{ds}^p(k+1), i_{qs}^p(k+1)$	
	Cost function Minimization	
6.	by using (22)	%Minimization of cost function
	min $J(k)$	
	Selection of reference currents and corresponding	
7.	rotor voltages	% Reference selection
	$i_r{}^* = i_{\alpha r}^* + j i_{\beta r}^*$	
	$v_r^* = v_{\alpha r}^* + j v_{\beta r}^*$	
8.	end	
	Extracting the magnitude and the angle of rotor	
9.	voltage	% Cartesian to polar transformation
	$\lvert v_r^* \rvert = \sqrt{{v_{\alpha r}^*}^2 + {v_{\beta r}^*}^2}$,	
	$\theta^* = \tan^{-1}\left(\frac{v_{\beta r}^*}{v_{\alpha r}^*}\right)$	
	Calculating the modulation	
10.	index m_a	% Modulation index
	$m_a = \frac{\sqrt{3}\lvert v_r^* \rvert}{v_{dc}}$	
	Determining the duty cycles	
11.	Ta	% Duty cycle
	Tb	
	T0	
12.	Apply the duty cycles to the PWM.	
13.	k = k+1 and go to line 3.	% go to next instant (k+1) and repeat…

32. G. F. Gontijo, T. C. Tricarico, B. W. França, L. F. d. Silva, E. L. v. Emmerik, and M. Aredes, "Robust Model Predictive Rotor Current Control of a DFIG Connected to a Distorted and Unbalanced Grid Driven by a Direct Matrix Converter," IEEE Transactions on Sustainable Energy, vol. 10, no. 3, pp. 1380-1392, 2019.
33. L. Riachy, H. Alawieh, Y. Azzouz, and B. Dakyo, "A Novel Contribution to Control a Wind Turbine System for Power Quality Improvement in Electrical Networks," IEEE Access, vol. 6, pp. 50659-50673, 2018.
34. Y. Zhang, T. Jiang, and J. Jiao, "Model-Free Predictive Current Control of DFIG Based on an Extended State Observer Under Unbalanced and Distorted Grid," IEEE Transactions on Power Electronics, vol. 35, no. 8, pp. 8130-8139, 2020.
35. M. A. Mossa, T. D. Do, A. S. Al-Sumaiti, N. V. Quynh, and A. A. Z. Diab, "Effective Model Predictive Voltage Control for a Sensorless Doubly Fed Induction Generator," IEEE Canadian Journal of Electrical and Computer Engineering, vol. 44, no. 1, pp. 50-64, 2021.
36. R. Errouissi, A. Al-Durra, S. M. Muyeen, S. Leng, and F. Blaabjerg, "Offset-Free Direct Power Control of DFIG Under Continuous-Time Model Predictive Control," IEEE Transactions on Power Electronics, vol. 32, no. 3, pp. 2265-2277, 2017.
37. W. Yunfei, Z. Xing, X. Zhen, and Y. Hui, "Model predictive direct current control of DFIG at low switching frequency," in 2016 IEEE 8th International Power Electronics and Motion Control Conference (IPEMC-ECCE Asia), 2016, pp. 1432-1435.
38. M. M. Vayeghan and S. A. Davari, "Torque ripple reduction of DFIG by a new and robust predictive torque control method," IET Renewable Power Generation, vol. 11, no. 11, pp. 1345-1352, 2017.
39. M. Wang, Y. Shi, Z. Zhang, M. Shen, and Y. Lu, "Synchronous Flux Weakening Control With Flux Linkage Prediction for Doubly-Fed Wind Power Generation Systems," IEEE Access, vol. 5, pp. 5463-5470, 2017.
40. S. Tohidi and M.-i. Behnam, "A comprehensive review of low voltage ride through of doubly fed induction wind generators," Renewable and Sustainable Energy Reviews, vol. 57, pp. 412-419, 2016/05/01/ 2016.
41. L. Xu, D. Zhi, and B. W. Williams, "Predictive Current Control of Doubly Fed Induction Generators," IEEE Transactions on Industrial Electronics, vol. 56, no. 10, pp. 4143-4153, 2009.
42. B. Q. V. Ngo, P. Rodriguez-Ayerbe, and S. Olaru, "Model Predictive Direct Power Control for doubly fed induction generator based wind turbines with three-level neutral-point clamped inverter," in IECON 2016 - 42nd Annual Conference of the IEEE Industrial Electronics Society, 2016, pp. 3476-3481.
43. Y. Venkata and W. Bin, "Chapter Appendices," in Model Predictive Control of Wind Energy Conversion Systems: IEEE, 2017, p. 1.
44. X. Lie and P. Cartwright, "Direct active and reactive power control of DFIG for wind energy generation," IEEE Transactions on Energy Conversion, vol. 21, no. 3, pp. 750-758, 2006.
45. T. Yifan and X. Longya, "A flexible active and reactive power control strategy for a variable speed constant frequency generating system," IEEE Transactions on Power Electronics, vol. 10, no. 4, pp. 472-478, 1995.